Experimental and Monte Carlo Simulation Studies on the Competitive Binding of Li+, Na+, and K+ Ions to DNA in Oriented DNA Fibers†

ARTICLE *in* THE JOURNAL OF PHYSICAL CHEMISTRY B · SEPTEMBER 1999

Impact Factor: 3.3 · DOI: 10.1021/jp9913517

4 AUTHORS, INCLUDING:

Nikolay Korolev
Nanyang Technological University
64 PUBLICATIONS **1,127** CITATIONS
SEE PROFILE

Alexander P Lyubartsev
Stockholm University
155 PUBLICATIONS **4,733** CITATIONS
SEE PROFILE

Experimental and Monte Carlo Simulation Studies on the Competitive Binding of Li^+, Na^+, and K^+ Ions to DNA in Oriented DNA Fibers†

Nikolay Korolev, Alexander P. Lyubartsev,‡ Allan Rupprecht, and Lars Nordenskiöld*

Arrhenius Laboratory, Division of Physical Chemistry, Stockholm University, S-106 91 Stockholm, Sweden

Received: April 26, 1999

Competitive binding of K^+, Na^+, and Li^+ to DNA was studied by equilibrating oriented DNA fibers with ethanol/water solutions in the range of ethanol concentration from 65 to 90% (by volume) and for salt concentrations, C_s, from 3 to 300 mM. The affinity of DNA for the cations decreases in the order Na ≈ K > Li, and this is opposite to the sequence determined for DNA in aqueous solution. The ion exchange equilibrium constant, $K_c^{K}_{Li}$, determined in the system DNA fibers−ethanol/water solutions of KCl and LiCl, varies between $K_c^{K}_{Li} \approx 1.4$ in 70% EtOH (K/Li = 1/1) and $K_c^{K}_{Li} \approx 2.5-2.7$ in 84−90% EtOH (K/Li = 1/1) or $K_c^{K}_{Li} \approx 3.7-4.0$ in 84% EtOH (K/Li = 1/9). Between 76 and 84% EtOH, the value of $K_c^{K}_{Li}$ increases steeply, which is due to the B−A transition of KDNA occurring in this concentration range of EtOH. Neither the A nor the B form of DNA exhibits selectivity for Na^+ or K^+ in mixtures of KCl and NaCl in ethanol/water solutions. Computer simulations based on the grand canonical Monte Carlo (GCMC) method were applied for modeling the experimental conditions. These calculations were performed within the approximations of describing the solvent as a dielectric continuum and the DNA polyion as a uniformly charged cylinder or a cylinder with arrays of spherical charges representing phosphate groups of the B or A form of DNA. It is found that the GCMC method explains qualitatively the ion selectivity of DNA in K/Li mixtures with respect to the dependence on the ethanol concentration, K/Li ratio, and A or B structural form of DNA.

Introduction

Most experimental and theoretical studies on the interactions between DNA and charged ligands (metal ions and complexes, DNA binding proteins, and other species) are made in dilute water solutions (see recent reviews).[1−3] However, in vivo, nucleic acids (RNA and DNA) are present as ordered condensed structures (i.e., chromatin, ribosomes) created by interactions with basic proteins, charged aliphatic amines, and metal ions. The driving forces of nucleic acid condensation are numerous,[4] but the decisive contribution to the thermodynamic stability of these structures is generally believed to come from electrostatic attraction between the negatively charged phosphate groups of DNA or RNA and the positively charged groups of basic proteins (rich in lysine and arginine amino acid residues) and other positively charged species (spermine^{4+}, spermidine^{3+}, Mg^{2+}).[4,5] Fluctuation-induced attractive correlation forces due to the presence of multivalent counterions is another important mechanism of DNA condensation.[4,6,7]

In dilute solutions, the DNA interaction with charged ligands, the helix−coil transition temperature, and other DNA properties are strongly dependent on the low molecular weight salt concentration.[1,2] At the same time, for condensed DNA states (fibers, gels) or in vivo, similar characteristics[8−10] are often independent of the ionic composition of the solvent. This discrepancy is usually explained by the direct and indirect consequences of the so-called macromolecular crowding effect (see ref 11 and references therein). It should be noted also that, in a condensed state of DNA (fiber, gel, liquid crystal), the mean concentration of counterions is very high (1−2 M), and this leads to loss of sensitivity of the binding and structural parameters of DNA on the concentrations of ions in the bulk solution. The concentrations of low molecular weight ions in chromatin should also be quite high because only about half of the total negative DNA charge is neutralized by net positive charge from the histone octamer. Thus, oriented fibers, gels, films, and liquid crystalline structures of DNA could serve as a basic model for describing the interactions between DNA and other ions in natural DNA states.

Available experimental data concerning the influence of monovalent cations and anions on the thermodynamic and kinetic parameters of biological polyelectrolyte systems indicate varying sensitivity of the studied processes to the nature of the charged low molecular weight species. It was found that the *lac*-repressor−DNA interactions[8] or the behavior of single-stranded DNA binding protein[12] showed only weak dependence on the nature of the cation but depended strongly on the nature of the anion. At the same time, the type of cation (Li^+, Na^+, or K^+) has a decisive influence on the equilibrium composition in the competitive reaction of interpolyelectrolyte complex formation.[13]

Thus, it is of importance to determine thermodynamic binding characteristics of monovalent ions in their interactions with

* To whom correspondence should be addressed. Fax: +46 8 15 2187. E-mail: lnor.physc.su.se.

† Abbreviations: AAS, atom absorption spectroscopy; CA, CB, uniformly charged cylinder model of the DNA polyion representing A- and B-DNA, respectively (see Figure 1); CC, counterion condensation; GCMC, grand canonical Monte Carlo; HA, HB, helical model of the DNA polyion representing A- and B-DNA, respectively (see Figure 1); $K_c^{K}_{M}$, $K_a^{K}_{M}$, apparent and corrected equilibrium constants of the ion exchange reaction (see eqs 2 and 3; M = Li or Na); MAS, magic angle spinning; MD, molecular dynamics; MSA, mean spherical approximation; PAAG, polyacrylamide gel; PB, Poisson Boltzmann; RDF, radial distribution function; RH, relative humidity.

‡ Also affiliated with the Scientific Research Institute of Physics, St. Petersburg State University, 198904 St. Petersburg, Russia.

10.1021/jp9913517 CCC: $18.00
Published on Web 09/30/1999

biological polyelectrolytes under conditions of high concentrations of the latter. Although studies of pure ionic forms of DNA in oriented fibers have provided a lot of valuable data (see refs 9 and 14−16 and references therein), the most clear understanding of differences between ions interacting with DNA could be obtained as a result of studying the direct competition of these ions in their binding to DNA. In the present work, we present results of experimental studies of competitive binding of Li^+, Na^+, and K^+ ions to DNA in oriented DNA fibers in ethanol/water solutions with various concentrations of ethanol (from 65 to 90% v/v) and salts (total salt concentrations C_s from 3 to 350 mM). DNA does not exhibit significant selectivity for K^+ or Na^+ in NaCl/KCl mixtures but preferentially binds K^+ from KCl/LiCl mixtures. It is found that the degree of DNA selectivity for K^+ depends on the concentrations of EtOH and salts, on the ratio K/Li, and on the DNA secondary structure. Furthermore, the B−A transition which occurs between 76 and 84% EtOH (v/v) enhances noticeably the preferential binding of K^+ from an equimolar mixture of KCl and LiCl. In addition, we also found that some amount of counterions in excess over the DNA phosphate can be absorbed into the DNA fibers when the salt concentration in the eluent exceeds 100 mM. We analyze available experimental and theoretical data that concern this accumulation of salt in the DNA phase.

One practical advantage of the ion exchange technique applied in the present study is of importance to point out. Data obtained in this way can be directly compared with the results of theoretical calculations based on the grand canonical Monte Carlo simulation approach. Most other experimental techniques cannot be compared directly with results from computer modeling, because of a gap between the detailed information obtained from the simulations and the output data of the experimental studies. Furthermore, the latter are often hard to interpret and usually demand assumptions in the theory of the method. For example, X-ray diffraction techniques allow only the localization of a small part of the most tightly bound ions and solvent molecules in the crystals of biological macromolecules.[17,18] NMR-based methods (e.g., ^{23}Na NMR relaxation[19−22]) produce information about relaxation times, and considerable theoretical model assumptions have to be invoked to obtain information about binding constants and other properties.[19]

In this work, we compare our experimental data with the results of grand canonical Monte Carlo (GCMC) simulations of a system of parallelly packed hexagonally arranged DNA polyanions of different structures, namely, uniformly and discretely charged polyions with the density and spatial distribution of the charged groups modeling A- or B-DNA. Our data reveal that the Monte Carlo approach with the approximation of a dielectric continuum and radii of the small ions obtained from modeling of simple electrolyte solutions can qualitatively and to some extent quantitatively explain the selectivity of DNA for Li^+, Na^+, and K^+ in oriented DNA fibers. However, we realize that the simulation model presented in this paper has numerous oversimplifications. Work is in progress in our laboratory to model competitive counterion binding in DNA fibers in a mixed ethanol/water solvent by means of the molecular dynamics simulation method.

Materials and Methods

High molecular weight salmon testes NaDNA (Fluka Chemie AG, Buchs, Switzerland) was used without further purification. Ethanol (99.5% v/v) was purchased from Kemetyl AB (Stockholm, Sweden). All ethanol concentrations quoted in this paper are given in percents by volume. Analytical grade Li-, Na-, and KCl were purchased from Merck KGaA (Darmstadt, Germany). Ultrapure KCl and spectrapure NaCl from Alfa (Johnson Matthey GmbH, Karlsruhe, Germany) were used for preparations of ionization buffers in AAS analyses.

Samples of highly oriented NaDNA fibers for ion exchange, X-ray diffraction, and mechanochemical studies were prepared by a wet spinning technique.[23,24] Methods of X-ray diffraction[25] and mechanochemical[9,26] measurements are described in detail in the references cited.

Ion Exchange Measurements. The conditions of wet spinning preparation of the samples for ion exchange measurements were similar to those applied in the sample preparations for NMR experiments.[15] The resulting samples had accurate orientation of the DNA polymeric chains as shown by the rotor-synchronized 2D magic angle spinning (MAS) ^{31}P NMR technique and by X-ray diffraction.[15] Samples for ion exchange experiments were obtained by cutting pieces from a fiber bundle. Each sample contained about 2−4 mg of DNA. The samples were then transferred to salt free ethanol/water mixtures of different EtOH concentrations and equilibrated in these mixtures for at least two weeks; NaCl admixtures were removed by replacement of salt free solution several times during the equilibration procedure. Then, 2−4 pieces of DNA fibers were transferred to tubes with solvent (eluent) of the same ethanol concentration but containing a mixture of KCl and LiCl or KCl and NaCl. To eliminate the influence of other metal cations and hydrogen ions, 0.05 mM $EDTA^{3-}$ was added to the eluents as K_3EDTA salt. The volume of eluent above the DNA samples was about 40 mL, and the amount of cations in the solvent was in great excess over the quantity of phosphate groups in the DNA fibers. Equilibrium concentrations of ions in the DNA fibers and in the eluent were reached by changing the solvent once a day during 7−10 days. Analysis of the last fraction of eluent in contact with DNA fibers was carried out, and it was found that the composition of this fraction never differed from that of the stock eluent.

When NaDNA fibers come into contact with the eluent containing a mixture of KCl and LiCl (or KCl and NaCl), an ion exchange reaction of Na^+ begins with substitution for a mixture of K^+ and Li^+ (or K^+ and Na^+). The composition of counterions neutralizing the phosphate groups of DNA depends on the thermodynamic affinity of DNA to these ions under the given conditions (temperature, solvent composition, and concentration of ions in the eluent).

The competition of K^+ with a second ion M^+ (M = Li or Na) can be written as the reaction

$$K^+(\text{eluent}) + \text{MDNA(fibers)} \leftrightarrow \text{KDNA(fibers)} + M^+(\text{eluent}) \quad (1)$$

with equilibrium constants

$$K_c^{K}{}_M = ([C_K]/[C_M])(C_M/C_K) \quad (2)$$

$$K_a^{K}{}_M = [C_K]/[C_M](a_M/a_K) = K_c^{K}{}_M(\gamma_M/\gamma_K) \quad (3)$$

Here $K_c^{K}{}_M$ is the apparent equilibrium or selectivity constant and $K_a^{K}{}_M$ is the so-called corrected selectivity constant since it is obtained after correction of $K_c^{K}{}_M$ for the preference of the solution phase, $[C_K]$, $[C_M]$, C_K, and C_M are, respectively, the concentrations of K^+ and M^+ in the DNA fibers and in the eluent, a_K, a_M, γ_K, and γ_M are the activities and activity coefficients of K^+ and M^+ in the eluent. The value of $K_c^{K}{}_M$ differs from the definition of the ion exchange competitive parameter D, which was proposed to measure the selectivity of

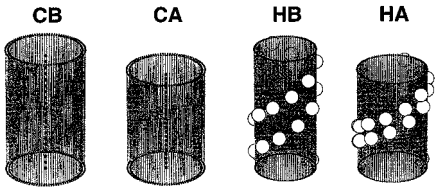

Figure 1. Models of the DNA polyion. CB, CA, HB, and HA are the abbreviations for the uniformly charged cylinder (CB, CA) or simplified helical (HB, HA) polyions mimicking A- and B-DNA, respectively. See the text for more details.

DNA−counterion interactions from ^{23}Na NMR relaxation studies.[27,28] This difference is because of the fact that the D values are based on the calculated relative amounts of counterions located in the close vicinity of the polyion whereas the total quantities of counterions in the DNA fiber phase are used in the determination of ${K_c}^{K}{}_{M}$ and ${K_a}^{K}{}_{M}$. However, the separation between the DNA polyions in condensed ordered fibers is very small, and thus every ion within the "DNA phase" can be considered as bound to the nearest polyion. Therefore, values of ${K_c}^{K}{}_{M}$ (or ${K_a}^{K}{}_{M}$) and the competitive parameter D can be directly compared.

The ion concentrations in eqs 2 and 3 have been determined experimentally as follows: After 7−10 days of equilibration with eluent, the DNA samples were quickly removed from the solvent, slightly pressed between sheets of weighing papers, weighed, and dried over phosphorus anhydride. The dried DNA samples were weighed again (to find the content of volatile components) and dissolved in bidistilled water. The concentrations of Li^+, Na^+, and K^+ in these DNA solutions were determined with a PU9100 AAS spectrometer (Phillips Scientific, Cambridge, Great Britain). To eliminate interference from the phosphate groups of DNA on the alkali metal atomic absorption, 0.2% (w/v) solutions of ultrapure potassium (as KCl) or sodium (as NaCl) solutions were used for the preparation of probes and standard solutions. The DNA concentrations, C_P, in the probes were determined by UV absorption measurements of acid-hydrolyzed DNA solutions.[29] We have preferred to use this method instead of the usual measurements at 260 nm because the secondary structure of DNA dissolved in pure water could be unstable,[30] which can introduce ambiguity in the extinction coefficient for DNA at 260 nm.

Grand Canonical Monte Carlo Simulation Method. *The Model*. We have used several models of the DNA polyion within our theoretical calculations of ion exchange properties. In the simplest model (cylindrical polyion), DNA was considered as an infinitely long uniformly charged hard cylinder of radius a and reduced linear charge density $\xi = l_b/b$, where b is the length of the cylinder corresponding to the unit charge and $l_b = e^2/\epsilon kT$ is the Bjerrum length ($l_b = 7.13$ Å for water at room temperature). For modeling of B-DNA, we have used the parameter values $a = 9.5$ Å and $b = 1.7$ Å (CB model in Figure 1); the corresponding values for A-DNA (CA model in Figure 1) are $a = 10$ Å and $b = 1.28$ Å. In the simulation program, we put negative unit charges on the polyion axis, so that they are separated by a distance b from each other (see Figure 1). Since $b \ll a$ and due to the Gauss theorem, such a charge distribution is equivalent to a uniform smearing of charge over the polyion surface. The radius a limits the area that is impenetrable for the centers of the smallest ion species. The larger ions cannot come closer to the polyion axis than $a_i = a + (\sigma_i - \sigma_{min})$, where σ_i and σ_{min} are the radii of the ith and smallest ion species.

Another model (helical polyion) was devised to incorporate the effects of the helical DNA grooves and the discrete charge localization on the DNA surface. This model has been used in previous papers.[7,31,32] The model has a hard cylindrical core of radius $a = 8$ Å for B-DNA (HB model in Figure 1) or $a = 9$ Å for A-DNA (HA model in Figure 1) and charged "phosphate groups" situated at the sites corresponding to the B or A form of DNA. The magnitude of a determines the distance of the closest approach to the polyion axis for the centers of all mobile ions. Each phosphate group has a charge $-e$ and a soft repulsive r^{-12} potential of effective radius $\sigma_- = 2$ Å. This set of phosphate groups forms an idealized model of double-stranded DNA with two grooves. Due to the repulsive short-range interactions, the average effective radius of DNA is about 10 Å for the B form and 11 Å for the A form.

In all the cases the ions are modeled as soft charged spheres of effective radius σ_i. The ions interact with each other and with the phosphate groups of DNA by the potential

$$V_{ij} = \frac{z_i z_j e^2}{4\pi\epsilon_0\epsilon r_{ij}} + kT\left(\frac{\sigma_i + \sigma_j}{r_{ij}}\right)^{12} \qquad (4)$$

(The first term is the Coulomb interaction of charges and the second is the "soft spheres" repulsion). The specific choice of ion radius σ_i for each ion type will be discussed below.

Simulation Details. The standard grand canonical Monte Carlo method[33] was employed in the simulations. The GCMC algorithm combines ordinary moves of particles in the simulation cell and steps with insertion or deletion of particles. The probabilities of the latter steps are defined by the chemical potentials of the species involved.[33] Thus, the GCMC algorithm reproduces statistical distributions corresponding to the grand canonical ensemble. This method is the natural choice to use for mimicking an experimental situation where the salt concentration inside the ordered DNA phase is not known. Instead this salt concentration is given by the thermodynamic constraint that the chemical potential in the ordered phase must be the same as in the bulk electrolyte phase. For each set of parameters, two simulations at equal chemical potentials have been performed: one for the ordered DNA phase and another for the bulk ion solution. Simulation of the bulk phase gives us bulk concentration of ions of each species corresponding to the given set of chemical potentials and also the ion activities from the relationship $\mu = kT \ln(\gamma C_M(h^2/2\pi mkT)^{3/2})$. A corresponding simulation of the ordered phase gives the distribution of ions in the ordered phase, which are in equilibrium with the bulk phase with a known bulk concentration of ions.

Since during the simulations the system should be kept electroneutral, steps with insertion or deletion of ions must be done by pairs of ions of opposite charge.[7,33] Normally, in a dense polyion system, the number of counterions in the cell greatly exceeds the number of co-ions; thus, exchange between different counterion species is hindered by the fact that co-ions must be involved in this process also. To facilitate the exchange between different species of counterions, we introduce another kind of Monte Carlo step, where one counterion is substituted by an ion of another type but of the same valency. This kind of step, being done according to the same rules for the grand canonical ensemble, accelerates greatly the process of approaching thermodynamic equilibrium between different ions of the same charge and is important for modeling ion exchange processes.

In all our simulations, we use a hexagonal simulation cell with DNA located along the z-axis and with periodic boundary conditions in all directions. Thus, we actually simulate an ordered DNA system.[7,31] The long-range part of the electrostatic interaction was taken into account by the Ewald method; details

TABLE 1: Parameters of the Simulation Cell Used in the GCMC Calculations

ethanol concn, % v/v	R,[a] Å	ϵ[b]	ethanol concn, % v/v	R,[a] Å	ϵ[b]
65	32	45	84	24.5	33.6
70	28	42	90	24	30
76	25	38.4			

[a] Determined from the data of ref 46. [b] Reference 39.

of its application are given in our previous work.[7] The height of the simulation cell was taken corresponding to the three full turns of DNA (102 Å for B-DNA and 84.48 Å for A-DNA). The size of the cell in the perpendicular direction typically corresponded to the distance between DNA in fibers (24−28 Å), but in some calculations it was greater. The total number of simulated ions varied from 100 to 400 depending on the salt concentration and the number of polyions in the simulation cell.

Dielectric Constant. The most common assumption used in polyelectrolyte theory calculations is the approximation of the solvent as a dielectric continuum. An alternative molecular description of the solvent around a polyion demands a tremendous increase of computer resources, and this has become available for systems of reasonable sizes only recently. Usually the dielectric constant, ϵ, of the pure solvent is used, and water is the solvent in the vast majority of calculations.

We carry out our experimental studies of DNA fibers in ethanol/water mixtures where the dielectric constant is substantially lower than in water (for example, $\epsilon = 30$ for 90% EtOH at 20 °C). Two circumstances, however, should be taken into account here. First, the ϵ value close to the polyion may differ substantially from the value determined in the pure solvent due to the ordering of solvent molecules, the high concentration of counterions, a lower value of ϵ inside the polyion, and other factors.[3,34,35] Second, double helical DNA exhibits hydrophilic properties, and the solvent inside the DNA fibers should be enriched with water. Data of ^{31}P NMR studies in water−organic solvents show that the phosphate groups in double helical polynucleotides are not sensitive to an increased concentration of the organic component in the solvent mixture.[36] This is an indirect indication that water remains the main constituent of the polynucleotide solvation shell independently of the presence of an organic component. This observation is confirmed by the results of MD calculations performed for a DNA oligomer in 85% EtOH.[37]

Consequently, there are mutually opposite factors which influence the value of ϵ inside the DNA fibers: enrichment of the DNA phase with water (this increases ϵ compared with that of the bulk solvent) and ordering solvent molecules in the strong electric field from the polyion, which produces a decrease of ϵ.[3,34,35] Unfortunately, determination of the ethanol content inside the DNA fibers (and in other ion exchangers) is a complex task, and so is the interpretation of the results.[38] In the absence of reliable experimental and/or theoretical evaluations of ϵ inside DNA fibers swollen in ethanol/water mixtures, we have used the values of ϵ determined in ethanol/water mixtures at 20 °C[39] (see Table 1).

Ionic Radii. A natural consequence of the dielectric continuum approximation is the introduction of "effective" radii of small ions and charged groups of the polyion to account for solvation effects. This is the only parameter which differs for the ions (Li^+, Na^+, K^+) in our model. Since the equilibrium concentrations of ions in the DNA fibers are defined by thermodynamic relationships, it is a natural choice to define the effective radii of ions from their thermodynamic properties. A couple papers[40,41] report values of monovalent ion radii obtained by fitting osmotic and activity coefficients, calculated within the MSA (mean sphere approximation) theory, to the corresponding experimental values. In this work we use ionic radii reported as the best fit values in recent MSA calculations,[41] which have taken into account the change of the dielectric constant of water close to the ions. Actually, only the best fit values of cation−anion separation are reported.[41] To evaluate the radii of individual ions, we have assumed equal hydration of K^+ and Cl^- in KCl solutions and obtained the following values of σ for Li^+, Na^+, K^+, and Cl^-, respectively: 2.35, 1.88, 1.62, and 2.00 Å.

We have also used the values of ionic radii obtained earlier by MSA calculations without correction for the ϵ change[42] and Stokes radii.[43] These two sets of ionic sizes gave much higher values of ion exchange constants, more clearly deviating from experimental data than the results obtained from the metal ion radii listed above. Therefore, we did not report values of $K_c^{K_M}$ calculated with parameters taken from those references.[42,43]

The existence of high local concentrations of phosphate groups and counterions in the vicinities of the DNA macromolecules allows us to consider the DNA fiber phase to be similar to a concentrated electrolyte solution. MD data show that, in concentrated electrolyte solutions ($C_s \approx 2$ M), cations and anions form dynamic ion pairs mostly of two sorts: contact, anion−cation, and solvent separated, anion−water−cation.[44,45] Consequently, the mean distance between neighboring ions of opposite charges lies somewhere between the values characteristic for these two sorts of ionic pairing, i.e., between the sum of their crystallographic radii and this sum plus the diameter of a water molecule. The above cited values of $\sigma_+ + \sigma_-$ lie just within this interval.

It should be pointed out here that we use ionic sizes determined in water solutions. The degree of ionic solvation can differ in ethanol/water mixtures especially at high ethanol content. Nevertheless, we believe our choice of ionic sizes to be reasonably correct and water to be the dominant solvating ligand in the DNA phase (see above).

The values of dielectric constants and DNA−DNA distances which we have used in the GCMC calculations are listed in Table 1. For evaluation of the DNA−DNA distance, R, in oriented fibers equilibrated in ethanol/water mixtures, we use the dependencies of R vs relative humidity (RH) determined in Na- and LiDNA fibers[46] and the analogy obtained by Wyckoff[47] for DNA fibers in ethanol/water mixtures and in air of different RH. He found that, in 85% EtOH, R was roughly the same as at 75% RH and in 70% EtOH roughly the same as at 92% RH.

Results and Discussion

GCMC Results for Oriented DNA in Simple Salt Solutions. Systems consisting of a polyelectrolyte and simple 1−1 salt in water solution have been extensively studied by a variety of theoretical models from simple counterion condensation (CC) theory to sophisticated MD techniques (see reviews).[1−3] However, the main topic of the majority of the theoretical publications is usually comparisons between different theoretical approaches. Relatively much attention has also been paid to the comparisons between polyelectrolyte theory predictions and experimental data on the competitive binding of counterions differing in charge, or to the polyelectrolyte aspects of interactions between DNA and molecules which are of interest from biochemical points of view (proteins and other biologically active substances). There are only a few publications concerning the differences in binding modes of counterions of various species but with the same charge.[1,28,48−51]

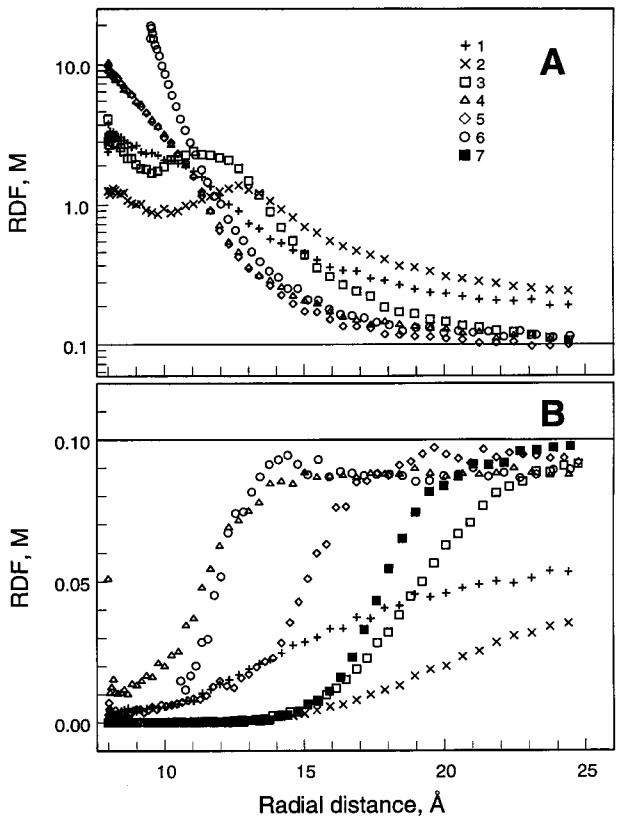

Figure 2. Dependencies of the RDF of counterions (A) and co-ions (B) on the distance from the polyion axis. Curves 1 and 2 are calculated for dielectric constant $\epsilon = 80.1$ (H_2O); curves 3−7 are for $\epsilon = 30$ (90% EtOH). Different polyion models were used: curves 1−5 are for the HB model, 6 and 7 are for the CB model. Different counterion and co-ion radii were also used: curves 1, 4, and 6 are for $\sigma_+ = 1$ and $\sigma_- = 2$ Å; curve 5 is for $\sigma_+ = 1$ and $\sigma_- = 5$ Å; curves 2, 3, and 7 are for $\sigma_+ = 3$ and $\sigma_- = 5$ Å. Other parameters are DNA−DNA distance, R, 50 Å ($C_P = 450$ mM), and bulk salt concentration, C_s, 100 mM (horizontal lines in the figures). Note the logarithmic scale of the ordinate in (A).

To check the possibilities of our GCMC model and to account for the effect of a decrease of the medium dielectric constant on the ion−polyion interactions, we have made some model calculations for a system consisting of a polyelectrolyte and 1−1 salt. In these calculations, the bulk concentration of the simple salt is taken equal to 100 mM, the DNA−DNA distance, R, is 50 Å ($C_P = 450$ mM for B-DNA), the ionic radii of the counterions and co-ions are $\sigma_+ = 1$ and 3 Å, $\sigma_- = 2$ and 5 Å, and the dielectric constants are either $\epsilon = 30$ (90% EtOH) or $\epsilon = 80.1$ (water at 20 °C). Calculated radial distribution functions (RDFs) are shown in Figure 2A for counterions and in Figure 2B for co-ions. The dependencies of RDF obtained for the HB model with $\sigma_+ = 3$ Å (curves 2 and 3 in Figure 2A) have two maxima: close to the polyion surface in the grooves (∼8 Å) and at $r = 11$ ($\epsilon = 30$) and 13 ($\epsilon = 80.1$) Å. These dependencies are in qualitative agreement with the RDF calculated for a recent simplified B-DNA model[32,52] and with the results of MD studies of NaDNA oligomers in water solution.[37,51,53,54] Our data confirm the earlier conclusion that the simplified presentation of the DNA polyion as a cylinder with spherical charges arranged in accordance with the DNA canonical structures is a good approximation for describing ion−ion interactions in polyelectrolyte systems.[32,52]

A change of the counterion size from 3 to 1 Å leads to the disappearance of the second maximum in the RDF curve and to a noticeable increase of the cation concentration near the polyion surface (curves 4 and 5 in Figure 2A). Analysis of the angular distribution of counterions around the HB model polyion shows that small cations ($\sigma_+ = 1$ Å) are collected preferably in the minor groove. The amount of counterions in this region is enough to neutralize the negative charges on the polyion to such an extent that they do not attract more cations to the vertexes of the phosphate groups. Cations with $\sigma_+ = 3$ Å have a more uniform angular distribution, they are not capable of reaching the bottom of the minor groove, and their concentration is high in the major groove and especially near the vertexes of the polyion's charges. Our results are in a general agreement with PB and Monte Carlo simulation data calculated in dependence on the counterion size for the all-atom presentation of poly(dGdC).[49] For the uniformly charged cylinder and $\epsilon = 30$, the distribution of counterions does not depend on the ionic size (in our model, the value of a limits the distance of the closest approach to the polyion axis for the centers of mobile ions). RDF calculated for $\sigma_+ = 1$ Å and $\sigma_- = 2$ Å is shown in Figure 2A (curve 6).

Decrease of the dielectric constant from 80.1 to 30 leads to a significant increase of the energies of ion−ion interactions. This causes mainly quantitative changes in the RDF curves of the counterions: the cation concentration increases 2−3 times within 2−3 Å around the polyion compared with the RDF calculated for $\epsilon = 80.1$ (compare curves 4 and 5 with 1 or curve 3 with 2 in Figure 2A). The distance where the cation concentration reaches bulk values becomes shorter at $\epsilon = 30$ than in water: for $\epsilon = 30$, this distance is approximately equal to 20 and 24 Å for $\sigma_+ = 1$ and 3 Å respectively; when $\epsilon = 80.1$ (curves 5 and 3 in Figure 2A), the concentration of counterions does not approach bulk values on the boundary of the simulation cell (curves 1 and 2 in Figure 2A).

The size of the co-ion does not influence the distribution of counterions: the RDFs obtained for $\sigma_+ = 1$ Å and $\sigma_- = 2$ or 5 Å level each other (curves 4 and 5 in Figure 2A). One can see by comparing parts A and B of Figure 2 that a decrease of the dielectric constant affects much more strongly the RDF curves of the co-ions than the RDF of the counterions. Small radii of counter- and co-ions lead to a noticeable increase of the co-ion concentration very close to the polyion surface ($r \approx$ 13−14 Å) for the CB model and $\epsilon = 30$: the RDF of anions has a local maximum in this region (curve 6 in Figure 2B). For the HB model and the same ionic sizes, the RDF of co-ions has no clear maximum at $r = 14$ Å, though the anion concentration is not negligible even near the very surface of the polyion (curve 4 in Figure 2B). For $\sigma_+ = 1$ Å and $\sigma_- = 5$ Å (HB model), the RDF of the co-ions is shifted about 3 Å from the polyion surface (curves 4 and 5 in Figure 2B). The increase of the radius of the counterions from 1 to 3 Å also leads to the expulsion of co-ions from the polyion (curves 3 and 2), and besides, this effect is more pronounced for the HB than for the CB model. Thus, for the HB model, an increase of both counter- and co-ion radii leads to a substantial shift of anions from the polyion: the RDFs of anions are approaching their bulk values (100 mM) at distances of 14−16 and 22−25 Å for these extreme cases (curves 4 and 3, respectively). The co-ion angular distribution (HB model) around the polyion shows that big anions (5 Å) have no significant angular dependence, while small anions (2 Å) are attached to the regions of high cation density and form a helical "cast" around the B-DNA minor groove.

Comparing our results with published data, we can note that the maximum of the co-ion RDF that we found for $\epsilon = 30$ and the CB model corresponds to results of the hypernetted chain

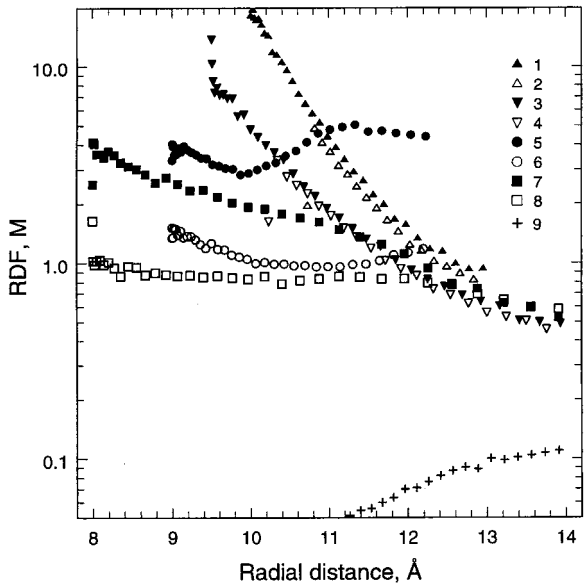

Figure 3. Dependencies of the RDF on the distance from the polyion axis calculated for competing counterions on the basis of ion exchange equilibria between DNA fibers and KCl/LiCl in ethanol/water solutions. Solid points are for K^+ ($\sigma_K = 1.62$ Å) (curves 1, 3, 5, and 7); empty points are for Li^+ ($\sigma_{Li} = 2.35$ Å) (curves 2, 4, 6, and 8); crosses are for Cl^- ($\sigma_{Cl} = 2.00$ Å). Curves 1−4 are for the uniformly charged cylindrical polyion models (1, 2, CA model; 3, 4, CB model), and curves 5−9 are for discretely charged polyion models (5, 6, HA model; 7−9, HB model). Other parameters are $R = 24.5$ Å and $\epsilon = 33.6$ (84% EtOH) (curves 1, 2, 5, and 6) and $R = 28$ Å and $\epsilon = 42$ (70% EtOH) (curves 3, 4, 7, and 8). Note the logarithmic scale of the ordinate.

model calculations, where a maximum in the co-ion RDF was found for solutions of polyelectrolyte in the presence of divalent counterions.[55] Similar results were obtained in Monte Carlo simulations of the system DNA + multivalent polyamine ions.[7] At low dielectric permittivity, enhancement of the ion−ion interaction makes the ion−ion correlation effects stronger, and the excess of co-ion accumulation can be observed also in the presence of monovalent counterions.

GCMC Simulation Results on the Competitive Binding of Counterions to DNA. Some RDFs of counterions calculated by the GCMC simulation method for parameters modeling ion exchange of K^+ and Li^+ in oriented fibers of DNA are shown in Figure 3. One can see that, for uniformly charged cylinder models of the DNA polyion, the RDF curves for small (K^+, $\sigma_+ = 1.62$ Å) and large (Li^+, $\sigma_+ = 2.35$ Å) ions come very close to each other (curves 1 and 3 for K^+ and the CA and CB models, respectively, curves 2 and 4 for Li^+ in the CA and CB models). The difference in the amount of Li^+ and K^+ ions calculated from RDF obtained for CB or CA models in the simulation cell is due to the ability of the smaller K^+ ions to approach more closely to the polyion axis. This difference determines the magnitude of the calculated values of $K_c^{K}{}_{Li}$, which appears to be quite close to the experimental data (see below). The similarity of the RDF curves, calculated for the counterions of equal charge but different size, provides also a simple way for determination of the amount of ions of each species associated with the charged cylinder: it is sufficient to calculate only one RDF curve for the smallest species and then integrate the curve (with proper normalizing factor), starting from the distance of minimum approach for this ion species.

The more realistic discretely charged polyion models (HB and HA, Figure 1) produce significantly different RDFs for small (K^+, $\sigma_+ = 1.62$ Å) as well as large (Li^+, $\sigma_+ = 2.35$ Å) ions competing near the DNA surface (see Figure 3, curves 5 and 7 for K^+ and the HA and HB models, respectively, curves 6 and 8 for Li^+ in the HA and HB models).

For a high concentration of salts in the bulk solution, the co-ions can penetrate into the ordered DNA phase. Curve 9 in Figure 3 shows an RDF of anions ($\sigma_- = 2$ Å) calculated for $C_s = 300$ mM, $C_K/C_{Li} = 1/1$, and $\epsilon = 42$. The presence of salts (K-, Li-, or NaCl) in the DNA fibers is also observed in ion exchange experiments, and the amount of sorbed salts is much higher than estimated from the GCMC method (see below).

We are aware of only a few theoretical determinations of RDFs and binding constants for systems of DNA plus competing counterions, where the counterions are of the same charge. Canonical Monte Carlo simulations have been carried out for monovalent counterions of very different sizes ($\sigma_+ = 0.5$ and 5 Å).[48] The role of the charge distribution on the polyion (continuous or discrete) was, however, not studied in that work.[48] It was only noted that representing the polyion as a uniformly charged cylinder or as a system of discrete charges did not influence the RDF of small counterions ($\sigma_+ = 0.5$ Å). Data of a ^{23}Na NMR study of the competition of Na^+ with other monovalent counterions (alkali metal and quaternary aliphatic amine cations) for binding to DNA have been compared with predictions of PB and GCMC models.[28] The DNA was modeled as an impenetrable cylinder of radius 10 Å with point charges arranged in a double helical array as in B-DNA, positioned 1 Å inside the surface of the cylinder (GCMC simulations), or as a uniformly charged cylinder (PB calculations). The radii of the counterions were taken to be equal to the Stokes values. A qualitative correspondence of theoretical (both PB and GCMC) and experimental data was found for all counterions with the exception of Li^+. Li^+ ions exhibit a higher ability than theoretically predicted to compete with Na^+ for binding to DNA.[28] The counterion competition coefficient D deviates from unity more noticeably when calculated by the GCMC method as compared to the PB approach. The authors[28] did not state whether this variance originated from the choice of theoretical model (PB or GCMC) or was due to the different descriptions of the polyion.

Comparisons of Experimental and GCMC Simulation Results. *Structural States of DNA in Oriented Fibers.* We have determined ion exchange properties of oriented DNA fibers equilibrated in 70, 76, 84, and 90% EtOH in the presence of a mixture of KCl and LiCl. The concentrations of KCl and LiCl in the eluents were equal, and the total salt concentration, C_s, was varied from 3 to more than 300 mM. Precipitation of salt is observed at high salt and EtOH concentrations, which limits the range of C_s studied in 76, 84, and 90% EtOH. In 84% EtOH, we have also studied the dependence of $K_c^{K}{}_{Li}$ on the ratio of K^+ and Li^+ in the eluent: this was varied approximately as $C_K/C_{Li} = 1/9$, 1/1, and 9/1. Experimental data on the K/Li system are collected in Table 2. Similar measurements were carried out for determination of $K_c^{K}{}_{Na}$ and $K_a^{K}{}_{Na}$ (results are in Table 3) in 65, 76, 84, and 90% EtOH for $C_K/C_{Na} = 1/1$ and C_s from 30 to 200 mM.

Detailed studies of the pure alkali metal salts of oriented DNA fibers were carried out earlier.[9,25] It was found that increasing the ethanol concentration in the bathing solution leads to the B−A transition between 70 and 80% EtOH for NaDNA and between 76 and 84% EtOH for KDNA. LiDNA was never found in the A form, and increasing the ethanol concentration and/or decreasing the LiCl concentration in ethanol/water mixtures lead to transformation of LiDNA from the B to C form.[9,25] The C form of DNA belongs to the B family of the DNA double helical structures,[56] although the detailed structural description of this

TABLE 2: Results of the Experimental Determination of the DNA Selectivity for K^+ and Li^+ in Oriented DNA Fibers Immersed in Ethanol/Water Solutions

ethanol concn, % v/v	K/Li ratio	C_s, mM	x_K[b]	$K_c^{K}{}_{Li}$	$\sum[C_M]/C_P$[c]	$\sum C_M/C_P$[d]	DNA secondary structure
70	1/1	3.87	0.483	1.82	1.05 ± 0.02	0.003	mixture of B and C forms
		32.4	0.500	1.63	1.02 ± 0.02	0.0015 ± 0.0005	
		108	0.497	1.42	1.18 ± 0.02	0.053 ± 0.006	
		351	0.498	1.55	1.50 ± 0.12	0.19 ± 0.03	
76	1/1	4.05	0.484	1.95	1.10 ± 0.05	0.003	mixture of B and C forms
		10.8	0.470	2.03	1.11 ± 0.06	0.005	
		32.8	0.497	1.75	1.14 ± 0.09	0.014	
		114	0.501	1.63	1.14 ± 0.03	0.045 ± 0.005	
84	1/1	4.40	0.475	2.50	1.01 ± 0.02	0.002	A form with some amount of the C form
		10.5	0.474	2.48	1.03 ± 0.02	0.005	
		33.7	0.496	2.22	1.07 ± 0.02	0.020 ± 0.005	
		104[a]	0.449	2.66	1.27 ± 0.02	0.060 ± 0.005	
	1/9	4.81	0.098	3.80	0.99 ± 0.06	0.003	C form, C_s = 10 mM; poor crystallinity
		11.95	0.096	3.38	1.11 ± 0.10	0.008	(mixture of C and P forms),
		38.4	0.094	3.27	0.98 ± 0.06	0.02	C_s = 300 mM
		118	0.097	3.00	1.06 ± 0.04	0.050 ± 0.005	
		332[a]	0.097	8.5	1.84 ± 0.10	0.15 ± 0.03	
	9/1	3.67	0.885	2.18	1.03 ± 0.02	0.002	A form
		10.5	0.883	2.14	0.98 ± 0.04	0.005	
		32.8[a]	0.890	1.90	1.05 ± 0.02	0.02	
90	1/1	4.40	0.493	2.60	1.18 ± 0.05	0.002	poor crystallinity
		10.6	0.493	2.41	1.12 ± 0.02	0.005	(mixture of A and P forms)
		33.8	0.491	2.29	1.25 ± 0.05	0.020 ± 0.005	

[a] Precipitation of salts in the eluent. [b] x_K = molar part of K^+ in the eluent. [c] $\sum[C_M]/C_P$ = relative amount of metal ions in the DNA fiber sample. [d] $\sum C_M/C_P$ = estimated sorption (relative to the DNA quantity, C_P) of metal ions from the eluent determined from the loss of mass of the DNA sample while drying. Other values listed in the table are defined in eqs 2 and 3.

TABLE 3: Results of the Experimental Determination of the DNA Selectivity for K^+ and Na^+ in Oriented DNA Fibers Immersed in Ethanol/Water Solutions with K/Na Ratio 1/1

EtOH content, % v/v	C_s, mM	x_K[b]	$K_c^{K}{}_{Na}$	$K_a^{K}{}_{Na}$	$\sum[C_M]/C_P$[c]	$\sum C_M/C_P$[d]	DNA secondary structure
65	30.9	0.482	1.00	1.08	1.06 ± 0.02	0.030 ± 0.005	
	103	0.491	0.93	1.04	1.13 ± 0.02	0.075 ± 0.005	B form, small amount of the A form
	154	0.492	0.96	1.07	1.17 ± 0.02	0.09 ± 0.01	
	207	0.493	0.93	1.08	1.25 ± 0.02	0.13 ± 0.02	
76	34.1	0.439	0.93	1.08	1.09 ± 0.02	0.020 ± 0.002	
	112	0.455	0.88	0.99	1.19 ± 0.03	0.075 ± 0.005	mixture of A and B forms
	170	0.454	0.88	1.04	1.25 ± 0.02	0.085 ± 0.015	
	219	0.457	0.88	1.10	1.32 ± 0.08	0.10 ± 0.03	
84	34.2	0.451	0.82	0.95	1.24 ± 0.05	0.018 ± 0.004	A form
	111[a]	0.444	1.70 ± 0.30	2.33 ± 0.40	1.85 ± 0.20	0.053 ± 0.015	
90	31.0	0.490	1.00	1.48	1.19 ± 0.02	0.02	A and P forms

[a] Precipitation of salts in the eluent. [b] x_K = molar part of K^+ in the eluent. [c] $\sum[C_M]/C_P$ = relative amount of metal ions in the DNA fiber sample. [d] $\sum C_M/C_P$ = estimated sorption (relative to the DNA quantity, C_P) of metal ions from the eluent determined from the loss of mass of the DNA sample while drying. Other quantities listed in the table are defined in eqs 2 and 3.

specific structural form of DNA still is uncertain.[15] In 90% EtOH, K- and NaDNA occur as a mixture of A and P forms, and LiDNA is a mixture of P and C forms. The so-called P form of DNA is a designation for a DNA structural state observed at high ethanol concentrations or in the air of low RH (below 60% for NaDNA). This form is characterized by strong aggregation between the DNA double helices, as well as by a substantial distortion of the base stacking and the helical regularity.

There are many similarities in the structural transitions of fibrous Na- and KDNA, and thus the structural state of DNA in mixed K/Na salt can be reliably predicted from the results of previous studies.[9] We list structural forms of DNA predicted for the K/Na system in the last column of Table 3. However, the structural state of DNA in mixed K/Li salt cannot be predicted because of the special properties of Li ions. Therefore, we determined the DNA structure in fibers equilibrated in 70, 84, and 90% EtOH with different concentrations and ratios of KCl and LiCl. We have compared mechanochemical properties of DNA fibers in mixed salt solutions with those determined in ethanol/water baths with pure KCl or LiCl.[9] We have also taken X-ray diffraction pictures of K/LiDNA fibers separated from ethanol solutions and equilibrated in air at RHs approximately corresponding to the ethanol concentrations of the baths from which these samples were extracted. Results obtained for DNA fibers in ethanol/water mixtures (mechanochemistry) and in air of different humidity (X-ray diffraction) are in good agreement with each other. These data show that Li^+ ions do not block the B−A transition in 84 and 90% EtOH solutions with C_K/C_{Li} = 1/1, although the X-ray diffraction patterns exhibit some presence of C-DNA in 84% EtOH and are of poor crystallinity in 90% EtOH due to the presence of the P form (it is also possible that higher scattering from K atoms deteriorates the quality of the X-ray pictures, which are not so clear in comparison with the same pictures of pure Na- or LiDNA).[15,25] For the K/Li ratio 1/9 in 84% EtOH, we have determined that K/LiDNA is in the C form at low salt concentration and in a mixture of P and C forms at high salt concentration. Data

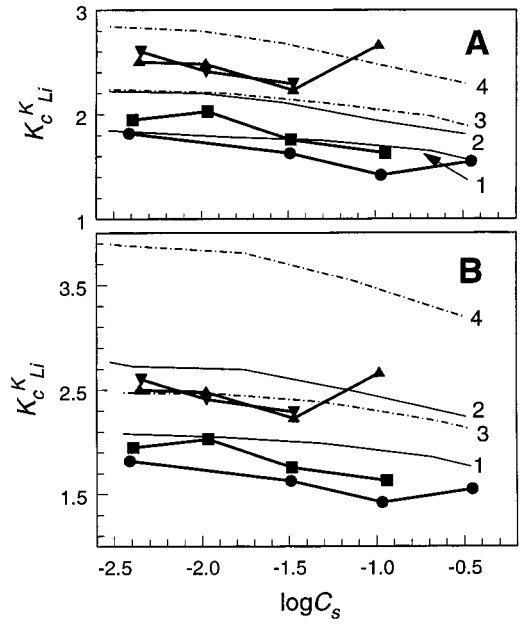

Figure 4. Dependencies of experimental (fat lines with solid points) and calculated for uniformly charged (A) and helical (B) polyions, values of $K_c{}^{K}{}_{Li}$ (thin lines with numbers) on the total salt concentration, C_s, in the eluents. All data are for $C_K/C_{Li} = 1/1$. Experimental data are marked as circles (70% EtOH), squares (76% EtOH), up triangles (84% EtOH), and down triangles (90% EtOH). Calculated values of $K_c{}^{K}{}_{Li}$ are obtained for models of B-DNA (thin solid lines) and A-DNA (thin dotted lines). $\epsilon = 42$ (70% EtOH) (curves 1 and 3) and $\epsilon = 30$ (90% EtOH) (curves 2 and 4).

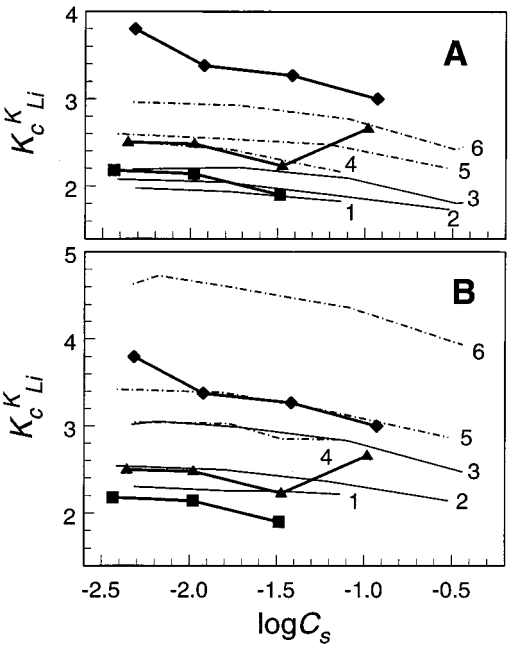

Figure 5. Dependencies of experimental (fat lines with solid points) and calculated, for uniformly charged (A) and helical (B) polyions, values of $K_c{}^{K}{}_{Li}$ (thin lines with numbers) on the total salt concentration, C_s, in 84% EtOH and at different C_K/C_{Li} ratios. Experimental data are marked as squares ($C_K/C_{Li} = 9/1$), triangles ($C_K/C_{Li} = 1/1$), and rhombi ($C_K/C_{Li} = 1/9$); theoretical curves are drawn as solid lines for the B-DNA (curves 1−3) and as dotted ones for the A-DNA (curves 4−6). Values of C_K/C_{Li} for the theoretical curves are the following: 9/1 (3, 6), 1/1 (2, 5), and 9/1 (1, 4).

obtained for the K/Li ratios 1/1 and 9/1 allow us to suggest that DNA is in the A form in 84% EtOH. Conclusions on the secondary structure of K/LiDNA are listed in the last column of Table 2.

Competitive Binding of Li^+ and K^+ Ions to DNA in Oriented Fibers. Results of the experimental studies on ion exchange properties of DNA fibers in ethanol/water solutions containing KCl + LiCl are summarized in Table 2 and compared with data of GCMC calculations in Figures 4 and 5. In these figures, experimental data are drawn as solid points and fat lines, calculated values of $K_c{}^{K}{}_{Li}$ as thin lines with numbers (data with precipitation of salt in the eluent not included; see Table 2). Taking into account that the accuracy of AAS measurements is considered to be about 5%, we estimate the maximal error of the $K_c{}^{K}{}_{Li}$ determinations to be about 10%. Experimental values of activity coefficients for KCl and LiCl in ethanol/water mixtures are available in the literature for all concentrations of KCl and for concentrations of LiCl up to 60−80 mM.[57] Values of $K_a{}^{K}{}_{Li}$ calculated by eq 3 using literature data on γ_{Li}/γ_K show no or little dependence on the salt concentration and are equal to or slightly higher than $K_c{}^{K}{}_{Li}$ obtained in $C_s = 3$ mM.

Experimental and calculated values of $K_c{}^{K}{}_{Li}$ vs log C_s are displayed in Figure 4 for $C_K/C_{Li} = 1/1$ and different EtOH concentrations (from 70 to 90%), and in Figure 5 for ratios $C_K/C_{Li} = 1/9$, 1/1, and 9/1 obtained in 84% EtOH. For simplicity, only curves calculated for border values of the dielectric constant $\epsilon = 42$ (70% EtOH) and $\epsilon = 30$ (90% EtOH) are shown in Figure 4. As can be seen from these figures and Table 2 there is a considerable selectivity of DNA for K^+ compared with Li^+ for all concentrations of EtOH (Figure 4) and all ratios of C_K/C_{Li} in 84% EtOH (Figure 5). In Figure 4, $K_c{}^{K}{}_{Li}$ has a minimal value of about 1.4 at $C_s = 100$ mM in 70% EtOH. It reaches the value 2.6 at $C_s = 3$ mM (log $C_s = -2.52$) in 90% EtOH, $C_K/C_{Li} = 1/1$, and about 3.8 at $C_s = 4.8$ mM (log $C_s = -2.32$) in 84% EtOH, $C_K/C_{Li} = 1/9$. At constant EtOH concentration, the values of $K_c{}^{K}{}_{Li}$ decrease slightly with increasing C_s. This behavior can be explained by γ_K decreasing more steeply than γ_{Li} with increasing ionic strength.

Values of $K_c{}^{K}{}_{Li}$ are similar in 70 and 76% EtOH and in 84 and 90% EtOH. Between 76 and 84% EtOH, an abrupt increase of $K_c{}^{K}{}_{Li}$ is observed (1.4−1.8 times; Figure 4). From mechanochemical and X-ray diffraction data, this change in $K_c{}^{K}{}_{Li}$ can be assigned to the B−A transition of DNA.

An increase of $K_c{}^{K}{}_{Li}$, observed in solutions with $C_K/C_{Li} = 1/9$ as compared with the values obtained for $C_K/C_{Li} = 1/1$ (Figure 5), can be explained by the well-known phenomenon in ion exchange chromatography of preferential sorption of the minor component from the eluent.[58] It should also be mentioned that this effect is very small if a weak competitor (Li^+) is present as an admixture to K^+ (i.e., for $C_K/C_{Li} = 9/1$).

Comparing experimental and calculated curves, one can draw the conclusion that the GCMC approach we have used produces a satisfactory qualitative description of the $K_c{}^{K}{}_{Li}$ dependence both on the salt concentration and on the ratio C_K/C_{Li}, as well as on the dielectric constant of the ethanol/water mixtures. This is confirmed by the following: (a) The experimentally observed increase of the DNA selectivity for K^+ with increasing EtOH concentration corresponds to an increase of $K_c{}^{K}{}_{Li}$ calculated by the GCMC method. (b) The abrupt increase of $K_c{}^{K}{}_{Li}$ observed in experiments with ethanol/water mixtures between 76 and 84% EtOH and corresponding to the B−A transition is in agreement with GCMC data which reveal that $K_c{}^{K}{}_{Li}$ calculated for the CA or HA model are 1.4−1.8 times higher than $K_c{}^{K}{}_{Li}$ obtained for the CB or HB model under similar conditions (Figure 4). (c) A change of C_K/C_{Li} leads to similar changes in the experimental and theoretical curves (see Figure 5). (d) An increase of the ionic strength leads to a gradual decrease of both experimental and theoretical values of $K_c{}^{K}{}_{Li}$.

The GCMC calculations with the less realistic (uniformly charged cylinder) CB and CA models of the DNA polyions (Figures 4A and 5A) give better agreement with experimental data than the theoretical values of $K_c^{K_{Li}}$ determined for the discretely charged helical HA and HB models (Figures 4B and 5B). Bearing in mind other approximations having been made within our approach (e.g., neglecting the molecular nature of the solvent and independence of the size of the mobile ions on ethanol concentration), we do not consider this to reflect a real physical phenomenon. It is possible that, for the HA and HB models, overestimated theoretical values of $K_c^{K_{Li}}$ have been obtained because our model does not take into account changes in the composition of the solvent and degree of hydration (solvation) of the charged groups and ions, which may take place in the DNA fibers and which may depend on the ethanol and salt concentrations in the eluent. Li^+ ions can be partially dehydrated with an increase of ethanol concentration or due to the small distance between DNA polyions in the fibers. While in our model K^+ ion has a radius close to its crystallographic value and cannot change much with changing the environment, the decrease of the effective size of Li^+ (not taken into account by the theory) can in effect reduce the experimental values of $K_c^{K_{Li}}$. At the same time, the approximation of the DNA as a uniformly charged cylinder leaves more space available for the mobile ions in the vicinity of the polyion than for the real discretely charged macromolecules. In the GCMC simulations, the only factor reflecting the increase of the ethanol concentration is the decrease of the dielectric constant. This decrease of the ϵ values leads to enhancement of the attractive electrostatic forces; thus, more counterions are attracted to the polyion (independent of the ion's radius). In contrast to the HA or HB model, Li^+ has more space to come close to the CB or CA cylinder, and this reduces the value of $K_c^{K_{Li}}$. Thus, the better quantitative agreement for the CA and CB models may be due to cancellation of errors in the description. More important is the fact that both theoretical models qualitatively reproduce the experimental trends due to an increase in ethanol and salt contents as well as upon transition from B- to A-DNA.

It should be noted that the values of $K_c^{K_{Li}}$ obtained for the CB or HB and CA or HA models are distinctly different from each other. A higher charge density and closer distance between neighboring charges on the polyion in the model of A-DNA enhance the selectivity for the smaller K^+ compared to B-DNA. This is seen in Figure 4, $\epsilon = 42$, curves 1 (CB and HB) and 3 (CA and HA); $\epsilon = 30$, curves 2 (CB and HB) and 4 (CA and HA), as well as in Figure 5. Reduction of the ϵ value gives a monotone rise of $K_c^{K_{Li}}$ which is steeper for A-DNA than it is for B-DNA.

For $C_K/C_{Li} = 1/1$, $C_s = 3$ mM, and $R = 28$ Å, we have calculated $K_c^{K_{Li}}$ values for $\epsilon = 80.1$ (data not shown), corresponding to the hypothetical situation of DNA fibers "soaked in water"; the results are close to the experimental curves obtained in ethanol/water mixtures at high ethanol concentrations ($\geq$70%). Clearly, corresponding experimental data for this situation cannot be obtained because of the solubility of DNA fibers in water. Therefore, the GCMC model of DNA fibers, which takes into account mostly electrostatic interactions, predicts that more bulky ions are *always* weaker competitors than the smaller ones in binding to a discretely charged polyion. Values of $\ln K_c^{K_{Li}}$ vs the reciprocal dielectric constant calculated by the GCMC method are shown in Figure 6 for the HB (curve 1) and HA (curve 2) models. As should be expected for a quantity dependent on the electrostatic energy, there is a linear dependency of $\ln K_c^{K_{Li}}$ vs $1/\epsilon$. The points obtained at $\epsilon = 42$ ($1/\epsilon = 0.024$) fall below the straight lines for both the HA and HB models. This may be due to an uncertainty in the DNA−DNA distance corresponding to this value of ϵ.[46,47]

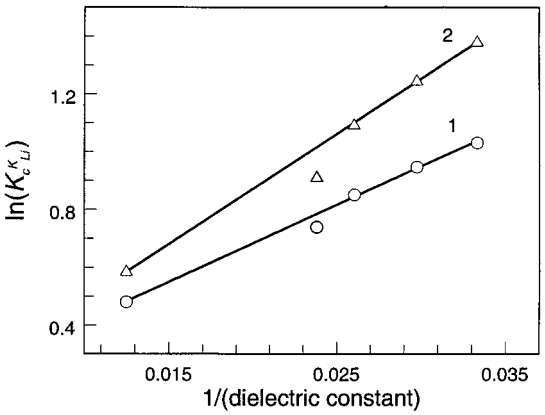

Figure 6. Dependencies of $K_c^{K_{Li}}$ calculated by the GCMC method on the reciprocal dielectric constant ($1/\epsilon$) of the eluent for the HB (1) and HA (2) models.

We have also determined the values of $K_c^{K_{Li}}$ for two other types of DNA models reported in the literature[28,32] for $\epsilon = 42$, $R = 28$ Å, and $C_K/C_{Li} = 1/1$ (data not shown). According to a model described in ref 32, we reduced the thickness of the cylinder to $a = 7$ Å and increased the distance from the polyion axis to the centers of the negative charges to 8.5 Å. Values of $K_c^{K_{Li}}$ obtained for this structure of the polyion are only slightly higher (5%) than the ones determined for our HB model under similar conditions. In another model,[28] the cylinder radius was set to 10 Å and the phosphate charges were fixed at 9 Å from the cylinder axis. The corresponding values of $K_c^{K_{Li}}$ became 5% lower compared to the results for the HB model.

Dependencies of $K_c^{K_{Li}}$ vs log C_s are shown in Figure 5 for different C_K/C_{Li} ratios. One can see that the rise of $K_c^{K_{Li}}$ with decreasing C_K/C_{Li} is well reproduced by the theory. However, mechanochemical and X-ray diffraction data reveal that DNA is not in the A form at $C_K/C_{Li} = 1/9$ but rather in the B or C forms with some contamination of the P form. At the same time, the curves 3 in Figure 5, calculated from the CB and HB models, both fall below the corresponding experimental curve (solid rhombi), and that is in contrast to all other data which place the theoretical values of $K_c^{K_{Li}}$ higher than the experimental ones. Possibly, the presence of the P form leads to a further increase of $K_c^{K_{Li}}$ if we assume that the more bulky Li^+ is a weaker competitor compared to the small K^+ in the highly aggregated P-DNA form. A structural description of P-DNA is not available (it is rather an abbreviation for a disordered DNA state caused by dehydration), and we are not aware of how this form could be approximated to fit in the polyelectrolyte theory calculations.

GCMC simulation results for the K/Li system, where Li^+ is assumed to be a larger ion than K^+, show that $K_c^{K_{Li}}$ is *always* larger than unity if the polyion is approximated as a system of discrete charges (see Figures 4−6). This prediction fits with experimental data obtained for DNA fibers immersed in ethanol/water mixtures. However, numerous indirect[27,30,59] and direct[60,61] experimental data on the interactions between DNA and Li^+ in aqueous solution show that Li^+ has some specific binding mode in its interaction with DNA. From a direct determination of $K_c^{K_{Li}}$ for DNA immobilized in a polyacrylamide gel (PAAG),[61] it is reported that these values are less than unity. However, the selectivity of DNA for Li^+ vanishes in water/organic mixtures. For DNA immobilized in PAAG, it was found that $K_c^{K_{Li}}$ became higher than unity when the water was replaced by a 50% dioxane/water mixture, i.e., when the DNA in PAAG was

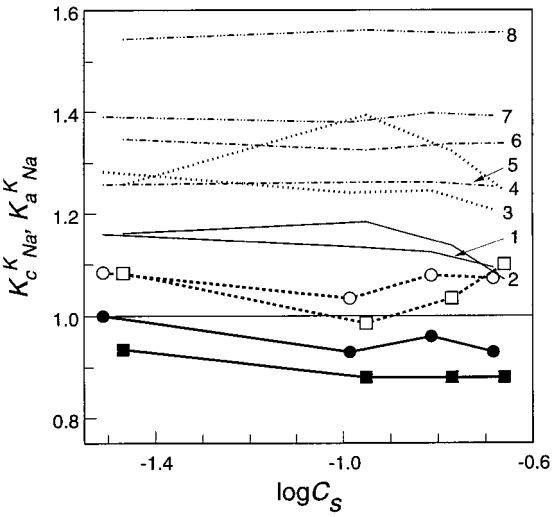

Figure 7. Dependencies of the experimental (fat lines with point symbols) and calculated (thin lines with numbers) values of $K_c^{K}{}_{Na}$ (fat symbols) and $K_a^{K}{}_{Na}$ (empty symbols) on the total salt concentration, C_s, for ion exchange equilibrium between DNA fibers and NaCl + KCl in ethanol/water solutions with a K/Na ratio of 1/1. Experimental data are marked as circles (65% EtOH) and squares (76% EtOH). Calculated values are given for $\epsilon = 45$ (65% EtOH) (curves 1, 3, 5, and 7) and $\epsilon = 38.4$ (90% EtOH) (curves 2, 4, 6, and 8). Curves 1 and 2 ($K_c^{K}{}_{Na}$) and 5 and 6 ($K_a^{K}{}_{Na}$) are for the HB model; curves 3 and 4 ($K_c^{K}{}_{Na}$) and 7 and 8 ($K_a^{K}{}_{Na}$) are for the HA model.

transferred into the condensed form. Consequently, specific binding of Li^+ preferably takes place when DNA is dissolved, while for DNA in the condensed state the binding properties of Li^+ can be better described by an electrostatic model. Thus, it may be concluded that DNA condensation and Li^+ site binding to DNA are competing processes. According to recent MD studies obtained in our laboratory,[51] Li^+ ions bind predominantly to DNA phosphate oxygen atoms and are capable of making stable ion pairs without disrupting water structure around DNA.

Competitive Binding of Na^+ and K^+ Ions to DNA in Oriented Fibers. Data on the relative DNA selectivity for K^+ and Na^+ are presented in Table 3. Experimental dependencies of $K_a^{K}{}_{Na}$ and $K_c^{K}{}_{Na}$ vs log C_s are compared in Figure 7 with the corresponding values calculated by the GCMC procedure. Curves with points are for experimental data; curves with numbers are the results of calculations. For NaCl and KCl in ethanol/water mixtures, available experimental data[57] show that the ratio γ_{Na}/γ_K, which determines the difference between $K_c^{K}{}_{Na}$ and $K_a^{K}{}_{Na}$ (eqs 2 and 3), increases with the concentrations of both ethanol and salt. It can be seen from Table 3 (columns 4 and 5) that correction of the counterion activities in the eluent leads to relatively small alterations of the values of $K_c^{K}{}_{Na}$ and $K_a^{K}{}_{Na}$. However, this correction places these constants on different sides of the value unity. Consequently, the introduction of the counterion activity leads to a qualitative change in the relative DNA selectivity for K^+ as compared to Na^+. Including this correction, the values of $K_c^{K}{}_{Na}$ which demonstrate a slight DNA selectivity for Na^+ can be explained by the lower activity of K^+ in ethanol solutions compared to the activity of Na^+. On the other hand, the error in the determination of the ion exchange constants is about 10% (from the accuracy of AAS measurements), and therefore it is fair to say that both $K_c^{K}{}_{Na}$ and $K_a^{K}{}_{Na}$ are equal to unity within the error of our method. DNA exhibits an unambiguous selectivity for K^+ only in 90% ethanol ($K_a^{K}{}_{Na} = 1.48$; see Table 3). The structural B−A transition which takes place between 70 and 85% ethanol for both pure K- and NaDNA[9] does not influence the DNA selectivity. It is possible that only strong aggregation and a partial transformation of A-DNA to the P form may lead to an increase of the selectivity for K^+ due to the smaller size of solvated K^+ ions (compared to Na^+).

In the GCMC calculations modeling K/Na competition, experimental activities of NaCl and KCl were used.[57] Comparison of experimental activities of Na^+ and K^+ with activities calculated by the GCMC method[31] in the absence of polyion show satisfactory agreement. It can be seen that the dependencies of $K_c^{K}{}_{Na}$ vs log C_s are not monotonic (curves 1 and 2 (HB) and 5 and 6 (HA) in Figure 6). Correction for nonideality of the eluent removes the dependencies of the ion exchange selectivity on the electrolyte concentration. This is in accordance with data obtained for sulfonic cation exchange resins in mixed solvents,[62] where the behavior of the selectivity constant was found to be due to changes of the activity coefficients of simple salts in the eluent. However, the range of the $K_c^{K}{}_{Na}$ change is much smaller for DNA fibers compared with synthetic ion exchangers[62] and is in the range of experimental error.

A decrease of the ϵ values leads to the increase of the magnitude of the theoretical values of $K_c^{K}{}_{Na}$ (left-hand sides of curves 4 and 2). This is in contrast with the experimental values of $K_c^{K}{}_{Na}$ showing a slight decrease with increasing ethanol concentrations. However, the observed differences in the values of $K_c^{K}{}_{Na}$ obtained in 65 and 76% ethanol lie close to the experimental uncertainty. Generally, the agreement between theoretical and experimental data seems to be satisfactory, given the experimental uncertainty and the approximations within the theoretical model.

Non Ion Exchange Sorption of Salts in DNA Fibers. In addition to the above results we have found yet another property of the DNA fibers equilibrated in the ethanol/water mixture with salt. It appears that the relative sum of cations, $\sum[C_M]/C_P$ (where $[C_M]$ and C_P are, respectively, the total molar amount of M^+ and phosphate groups in the sample of DNA fibers), becomes considerably higher than unity at high salt concentrations (usually at $C_s > 100$ mM). This means that some amount of salt is sorbed in the DNA fibers. The effect is relatively small for the K/Li system (column 6 of Table 2) but more significant in the K/Na system (column 6 of Table 3). In the seventh columns of Tables 2 and 3, we list the values of $\sum C_M/C_P$, where C_M is the amount of M^+ (due to added salt only) obtained for the DNA samples if one assumes that the concentration of salts in the solvent which soaks the DNA fibers is equal to the concentration in the eluent (which may be considered as the maximum amount sorbed). By subtraction of 1 from the entries in column 6, these values can be compared with the numbers in column 7. The amount of solvent in the swollen DNA fibers (the loss of sample weight in drying over P_2O_5) varied between 30 and 60%. This means that there was only a relatively small amount of solvent occupying the void space (dead volume) in the DNA fibers. Thus, most of the solvent is affected by the electric field from the highly charged DNA double helices, and simple salt (co-ions) should be largely excluded from this volume. In reality, such uneven distribution of salt as the maximum should not appear since the distribution of salt between the ordered phase and the outside bulk phase will be determined by the condition of equal chemical potential of all ionic species in the two phases.[63] This equilibrium is included in the GCMC calculations (see Figure 2B and curve 9 in Figure 3), but the effect is, however, much smaller than that observed in column 6 of Tables 2 and 3 (see below). Although the observed effect is close to the limit of reliability of our measurements, we consider that it is not a systematic error but

a real phenomenon. An interesting feature of the observed non ion exchange accumulation of salts in DNA fibers is the sensitivity to the nature of the cation: the quantity of MCl (M = Li, Na, or K) is substantially lower in the K/Li system than in the presence of K^+ or Na^+ (see Tables 2 and 3). Analysis of earlier data obtained for pure ionic forms of DNA showed that NaDNA fibers bathed in 73% ethanol with 0−0.22 M NaCl absorbed about 1.45 times more salt on a molar basis than did LiDNA fibers bathed with the same concentration of LiCl.[25] The phenomenon of nonequivalent sorption of simple salts is known in ion exchange chromatography.[64,65]

Two basic explanations of the salt accumulation in the DNA fibers may be proposed. First, overstoichiometric sorption of cations can be the consequence of a redistribution of salt between the eluent and the DNA fibers due to substantial enrichment of water in the DNA phase. This could lead to an increase of the salt concentration in the phase with more favorable solvation environment for ions such as in the case of the well-known redistribution of electrolytes between water and organic nonpolar solvents. The second explanation is based on the significant reduction of volume affected by the negative potential from the polyion with increasing C_s and lowering of the dielectric constant (curves in Figure 2B). Although this behavior of polyelectrolytes has been known for many years,[64,65] detailed experimental and theoretical studies of its role in polyelectrolytes (especially DNA) have not been carried out.

The GCMC method includes the conditions of equilibrium between the DNA and bulk phases, and the calculations show that a considerable amount of co-ions is collected in the cell occupied by the polyion for $R = 50$ Å and $C_s > 100$ mM (more than 100% of the amount of charged groups of the polyion). However, this quantity reduces to only 3−5% (at $C_s = 300$ mM) in calculations where DNA−DNA distances were equal to those listed in Table 1 (see also curve 9 in Figure 3). Values of non ion exchange sorption obtained in experiments are much higher than the values calculated by the GCMC method (see Tables 2 and 3). It has been shown[7] that, for $C_s > 100$ mM, the amount of co-ions in the cell occupied by DNA polyions is not negligible for DNA−DNA distances of 30−50 Å.

Concluding Remarks

Experimental studies of competitive binding of K^+, Na^+, and Li^+ to DNA in oriented fibers equilibrated in ethanol/water solutions show that the affinity of DNA to these cations decreases in the order Na ≈ K > Li, which is opposite the sequence determined for DNA and other polyelectrolytes with phosphate cation exchange groups in aqueous solution.[60,61,66] Li^+ ions placed in ethanol/water medium lose their ability to bind specifically to DNA in the form of oriented fibers. Li^+−DNA interactions can be qualitatively described by the electrostatic model in this case (in this work, by the GCMC simulation method).

Between 76 and 84% EtOH, the selectivity for K^+ increases steeply in a mixture of K^+ and Li^+, which is due to the B−A transition of KDNA occurring in this concentration range of EtOH. Neither the A nor the B form of DNA exhibits selectivity for Na^+ or K^+ in mixtures of KCl and NaCl in ethanol/water solutions. Our data on the DNA affinities for the alkali metal ions obtained for DNA oriented fibers in ethanol/water mixtures are in general agreement with the results of the studies of DNA[61] and other phosphate polyelectrolyte solutions and ion exchangers[22,60,66−68] obtained in water and in water/organic solvents. These studies report that an increase of the organic component in the eluent leads to a change of the metal ion selectivity order.

The GCMC simulation approach explains qualitatively the selectivity of DNA in K/Li mixtures, and how this selectivity depends on the ethanol concentration, K/Li ratio, and A or B structural form of DNA. The major approximation in our model is the treatment the solvent as a dielectric continuum. In the past few years, MD simulations have made great progress in describing ion−DNA interactions as well as structural properties of DNA (see refs 3, 14, 35, 51, and 53 and references therein). Investigations using the MD approach to obtain data on the ion exchange equilibrium constants in DNA fibers equilibrated in salt ethanol/water mixtures will be performed in our laboratory.

On the whole, our experimental data and theoretical calculations reveal that DNA fibers do not possess any particular selectivity for K^+ or for Na^+. In this context it is of interest to consider this result in relation to the distribution of Na^+ and K^+ in vivo. Na^+ and K^+ are slightly different in ionic sizes and behave differently in their interaction with water molecules. These differences have been suggested as the origin of the selective permeability of the cell membrane.[69,70] If one considers a cell as a small grain of ion exchange resin, then the values of $K_c^K{}_{Na}$ for this "ion exchanger" are equal to 600 or higher, when calculated from the mean concentrations of Na^+ and K^+ in extracellular liquids (seawater, blood serum) and intracellular fluid.[69] Phosphate groups of polymeric RNA and DNA are dominant anions in bacteria which are mainly responsible for the amounts of low molecular weight cations in bacteria[71] or in the eucaryotic cell nucleus. Some researchers consider the uneven Na/K distribution between the cell and its environment to be a consequence of a high thermodynamic affinity of the polyelectrolytes of the cell for K^+ ions (see ref 72 and references therein). Our data do not support this hypothesis, and no special selectivity of highly ordered aggregated DNA for K^+ (which has some features of the organization of DNA in vivo) is found.

Acknowledgment. This work has been supported by the Swedish National Science Foundation (NFR), the Royal Academy of Sciences (KVA), the Swedish Institute, and the Magn. Bergvall Foundation.

References and Notes

(1) Anderson, C. F.; Record, M. T., Jr. *Annu. Rev. Biophys. Biophys. Chem.* **1990**, *19*, 423.
(2) Anderson, C. F.; Record, M. T., Jr. *Annu. Rev. Phys. Chem.* **1995**, *46*, 657.
(3) Jayaram, B.; Beveridge, D. L. *Annu. Rev. Biophys. Biomol. Struct.* **1996**, *25*, 367.
(4) Bloomfield, V. A. *Curr. Opin. Struct. Biol.* **1996**, *6*, 334.
(5) Mirzabekov, A. D.; Rich, A. *Proc. Natl. Acad. Sci. U.S.A.* **1979**, *76*, 1118.
(6) Schmitz, K. S. *Acc. Chem. Res.* **1996**, *29*, 7.
(7) Lyubartsev, A. P.; Nordenskiöld, L. *J. Phys. Chem.* **1995**, *99*, 10373.
(8) Ha, J. H.; Capp, M. W.; Hohenwalter, M. D.; Baskerville, M.; Record, M. T., Jr. *J. Mol. Biol.* **1992**, *228*, 252.
(9) Rupprecht, A.; Piskur, J.; Schultz, J.; Nordenskiöld, L.; Song, Z.; Lahajnar, G. *Biopolymers* **1994**, *34*, 897.
(10) Schultz, J.; Rupprecht, A.; Song, Z.; Piskur, J.; Nordenskiöld, L.; Lahajnar, G. *Biophys. J.* **1994**, *66*, 810.
(11) Zimmerman, S. B.; Murphy, L. D. *FEBS Lett.* **1996**, *390*, 245.
(12) Lohman, T. M.; Overman, L. B.; Ferrari, M. E.; Kozlov, A. G. *Biochemistry* **1996**, *35*, 5272.
(13) Izumrudov, V. A.; Kargov, S. I.; Zhiryakova, M. V.; Zezin, A. B.; Kabanov, V. A. *Biopolymers* **1995**, *35*, 523.
(14) Piskur, J.; Rupprecht, A. *FEBS Lett.* **1995**, *375*, 174.
(15) Song, Z.; Antzutkin, O. N.; Lee, Y. K.; Shekar, S. C.; Rupprecht, A.; Levitt, M. H. *Biophys. J.* **1997**, *73*, 1539.
(16) Starikov, E. B. *Phys. Rep.* **1997**, *284*, 1.
(17) Chandrasekaran, R.; Radha, A.; Park, H. S. *Acta Crystallogr., Sect. D* **1995**, *51*, 1025.
(18) Luger, K.; Mader, A. W.; Richmond, R. K.; Sargent, D. F.; Richmond, T. J. *Nature* **1997**, *389*, 251.
(19) Chen, S. W.; Rossky, P. J. *J. Phys. Chem.* **1993**, *97*, 10803.

(20) Schultz, J.; Nordenskiöld, L.; Rupprecht, A. *Biopolymers* **1992**, *32*, 1631.
(21) Andreasson, B.; Nordenskiöld, L.; Eriksson, P.-E.; Rupprecht, A. *Biopolymers* **1994**, *34*, 1605.
(22) Braunlin, W. H.; Anderson, C. F.; Record, M. T., Jr. *Biopolymers* **1986**, *25*, 205.
(23) Rupprecht, A. *Acta Chem. Scand.* **1966**, *20*, 494.
(24) Rupprecht, A. *Biotechnol. Bioeng.* **1970**, *12*, 93.
(25) Rupprecht, A.; Forslind, B. *Biochim. Biophys. Acta* **1970**, *204*, 304.
(26) Rupprecht, A.; Piskur, J. *Acta Chem. Scand., Ser. B* **1983**, *37*, 863.
(27) Bleam, M. L.; Anderson, C. F.; Record, M. T., Jr. *Proc. Natl. Acad. Sci. U.S.A.* **1980**, *77*, 3085.
(28) Paulsen, M. D.; Anderson, C. F.; Record, M. T., Jr. *Biopolymers* **1988**, *27*, 1249.
(29) Spirin, A. S. *Biochemistry (Moscow)* **1958**, *23*, 656.
(30) Korolev, N. I.; Vlasov, A. P.; Kuznetsov, I. A. *Biopolymers* **1994**, *34*, 1275.
(31) Lyubartsev, A. P.; Nordenskiöld, L. *J. Phys. Chem. B* **1997**, *101*, 4335.
(32) Montoro, J. C. G.; Abascal, J. L. F. *J. Chem. Phys.* **1995**, *103*, 8273.
(33) Valleau, J. P.; Cohen, L. K. *J. Chem. Phys.* **1980**, *72*, 5935.
(34) Lamm, G.; Pack, G. R. *J. Phys. Chem. B* **1997**, *101*, 959.
(35) Young, M. A.; Jayaram, B.; Beveridge, D. L. *J. Phys. Chem. B* **1998**, *102*, 7666.
(36) Lerner, D. B.; Becktel, W. J.; Everett, R.; Goodman, M.; Kearns, D. R. *Biopolymers* **1984**, *23*, 2157.
(37) Sprous, D.; Young, M. A.; Beveridge, D. L. *J. Phys. Chem. B* **1998**, *102*, 4658.
(38) Demirgian, J.; Kishk, F.; Yang, R.; Marinsky, J. A. *J. Phys. Chem.* **1979**, *83*, 2743.
(39) Åkerlöf, G. *J. Am. Chem. Soc.* **1932**, *54*, 4125.
(40) Fawcett, W. R.; Tikanen, A. C. *J. Phys. Chem.* **1996**, *100*, 4251.
(41) Simonin, J.-P.; Blum, L.; Turq, P. *J. Phys. Chem.* **1996**, *100*, 7704.
(42) Triolo, R.; Grigera, G. R.; Blum, L. *J. Phys. Chem.* **1976**, *80*, 1858.
(43) Robinson, R. A.; Stokes, R. H. *Electrolyte solutions*, 2nd ed.; Butterworths: London, 1965.
(44) Lyubartsev, A. P.; Laaksonen, A. *J. Phys. Chem.* **1996**, *100*, 16410.
(45) Lyubartsev, A. P.; Laaksonen, A. *Phys. Rev. E* **1997**, *55*, 5689.
(46) Lindsay, S. M.; Lee, S. A.; Powel, J. W.; Weidlich, T.; DeMarco, C.; Lewen, G. D.; Tao, N. J.; Rupprecht, A. *Biopolymers* **1988**, *27*, 1015.
(47) Wyckoff, H. W. Thesis, Massachusetts Institute of Technology, Boston, 1955.
(48) Le Bret, M.; Zimm, B. *Biopolymers* **1984**, *23*, 271.
(49) Lamm, G.; Wong, L.; Pack, G. R. *Biopolymers* **1994**, *34*, 227.
(50) Rouzina, I.; Bloomfield, V. A. *Biophys. Chem.* **1997**, *64*, 139.
(51) Lyubartsev, A. P.; Laaksonen, A. *J. Biomol. Struct. Dyn.* **1998**, *16*, 579.
(52) Montoro, J. C. G.; Abascal, J. L. F. *J. Chem. Phys.* **1998**, *109*, 6200.
(53) Young, M. A.; Ravishanker, G.; Beveridge, D. L. *Biophys. J.* **1997**, *73*, 2313.
(54) Young, M. A.; Jayaram, B.; Beveridge, D. L. *J. Am. Chem. Soc.* **1997**, *119*, 59.
(55) Bacquet, R.; Rossky, P. J. *J. Phys. Chem.* **1988**, *92*, 3604.
(56) Arnott, S.; Selsing, E. *J. Mol. Biol.* **1975**, *98*, 265.
(57) Activities and activity coefficients of Li-, Na-, and KCl ethanol/water solution were taken from the following: Yang, R.; Demirgian, J.; Solsky, J. F.; Kikta, E. J., Jr.; Marinsky, J. A. *J. Phys. Chem.* **1979**, *83*, 2752. Mazzarese, J.; Popovich, O. *J. Electrochem. Soc.* **1983**, *130*, 2032. Dill, A. J.; Itzkowitz, L. M.; Popovich, O. *J. Phys. Chem.* **1968**, *72*, 4580. Popovich, O.; Gibofsky, A.; Berne, D. H. *Anal. Chem.* **1972**, *44*, 811.
(58) Goldring, L. S. In *Ion-exchange*; Marinsky, J. A., Ed.; Edward Arnold, Ltd., Marcel Dekker, Inc.: London, New York, 1966; pp 205−226.
(59) Manning, G. S. *Q. Rev. Biophys.* **1978**, *11*, 179.
(60) Strauss, U. P.; Helfgott, C.; Pink, H. *J. Phys. Chem.* **1967**, *71*, 2550.
(61) Kuznetsov, I. A.; Gorshkov, V. I.; Ivanov, V. A.; Kargov, S. I.; Korolev, N. I.; Filippov, S. M.; Khamisov, R. K. *React. Polym.* **1984**, *3*, 37.
(62) Fessler, R. G.; Strobel, H. A. *J. Am. Chem. Soc.* **1963**, *67*, 2567.
(63) Guldbrand, L.; Nilsson, L. G.; Nordenskiöld, L. *J. Chem. Phys.* **1986**, *85*, 6686.
(64) Reichenberg, D. In *Ion-exchange*; Marinsky, J. A., Ed.; Edward Arnold, Ltd.: London, 1966; pp 227−276.
(65) Dimond, R. M.; Whitney, D. C. In *Ion-exchange*; Marinsky, J. A., Ed.; Edward Arnold, Ltd.: London, 1966; pp 277−352.
(66) Bare, W.; Nordmeier, E. *Polym. J.* **1996**, *28*, 712.
(67) Nordmeier, E. *Macromol. Chem. Phys.* **1995**, *196*, 1321.
(68) Nordmeier, E. *Makromol Chem., Macromol. Symp.* **1992**, *61*, 114.
(69) Collins, K. D. *Biophys. J.* **1997**, *72*, 65.
(70) Doyle, D. A.; Cabral, J. M.; Pfuetzner, R. A.; Kuo, A.; Gulbis, J. M.; Cohen S. L.; Chait, B. T.; MacKinnon, R. *Science* **1998**, *280*, 69.
(71) Record, M. T., Jr.; Courtenay, E. S.; Cayley, D. S.; Guttman, H. J. *Trends Biochem. Sci.* **1998**, *23*, 143.
(72) Ling, G. N. *Physiol. Chem. Phys. Med. NMR* **1994**, *26*, 121.